

In Vitro Fatigue and Fracture Resistance of One- and Two-Piece CAD/CAM Zirconia Implant Abutments

Peter Gehrke, Dr Med Dent¹/Dirk Johannson, Dr Med Dent, MSc²/Carsten Fischer, MDT³/
Bogna Stawarczyk, Dr Rer Biol Hum, Dipl Ing, MSc⁴/Florian Beuer, Prof Dr Med Dent⁵

Purpose: All-ceramic abutments are employed increasingly often in implant dentistry for esthetic reasons. In vitro stress testing is required to evaluate the suitability of these constructions, especially in load-bearing posterior regions. The purpose of the study was to assess and compare the fatigue and fracture resistance of one- and two-piece computer-aided design/computer-assisted manufacture (CAD/CAM) zirconia implant abutments with an internal-hex connection and prefabricated commercially available zirconia stock abutments.

Materials and Methods: Twenty-one abutment-crown specimens were prepared for three test groups. Control group 1 (SZ) included specimens with unprepared stock zirconia abutments, test group 2 (OP) included one-piece CAD/CAM zirconia abutments, and test group 3 (TP) included two-piece CAD/CAM zirconia abutments. All 21 specimens underwent thermocycling and fatigue testing. Finally, all specimens were tested for fracture resistance with a universal testing machine. The maximum load was applied to the tapered occlusal area of each crown at a 30-degree angle and a crosshead speed of 0.5 mm/min until the implant–abutment connection failed. Kolmogorov-Smirnov, Shapiro-Wilk, and post-hoc Scheffé tests were used for statistical analysis.

Results: All abutments in groups SZ and OP fractured into two or more pieces after fracture resistance testing. None of the TP abutments displayed apparent disintegration, but failure was evidenced by bending of the retention screw. OP abutments (232.1 ± 29.8 N) and SZ abutments (251.8 ± 23.2 N) showed lower fracture loads than the TP abutments (291.4 ± 27.8 N). However, only the difference between the OP and TP groups was statistically significant. Further load-displacement analyses corroborated the higher mechanical stability of the TP abutments. **Conclusion:** Superior resistance was achieved for two-piece hybrid CAD/CAM zirconia abutments. These abutments might be clinically beneficial in high-load areas, such as premolar and molar regions. INT J ORAL MAXILLOFAC IMPLANTS 2015;30:546–554. doi: 10.11607/jomi.3942

Key words: ceramics, computer-aided design/computer-assisted manufacture, dental stress analysis, fracture load, hybrid abutments, elasticity, implant abutments, zirconia

Implant dentistry has evolved from an experimental method to a routine treatment option for the rehabilitation of edentulous and partially edentulous patients. Contemporary surgical and restorative techniques have been extensively researched and tested, with excellent functional and esthetic results.^{1–5}

The initial challenge of therapy—safe, durable osseointegration of the implant itself—has been

sufficiently addressed by a combination of technical developments, increasing research, and clinical experience.⁵ Because of this and as a consequence of increasing expectations of patients, additional criteria, primarily esthetic aspects, have gained increasing attention. The ultimate goal is a functional result with a pleasing smile architecture that considers the proper proportions and natural relationships among the peri-implant mucosa, underlying bone, and restorative materials.^{6,7} In addition to its esthetic relevance, the soft tissue around the dental implants serves as a protective barrier between the oral cavity and peri-implant bone.^{8,9} The surrounding mucosa is recurrently challenged by numerous hazards that can have adverse effects on implant longevity, such as plaque, mechanical loading, and prosthetic interference. The abutment material, which is in direct contact with this critical transition zone, appears to be decisive in ensuring a high-quality attachment between the mucosa and the abutment surface.¹⁰ Titanium, precious alloys,

¹Private Practice, Ludwigshafen, Germany.

²Private Practice, Bad Homburg, Germany.

³Laboratory Technician, Sirius Ceramics, Frankfurt, Germany.

⁴Material Scientist, Ludwig-Maximilians University Munich, Department of Prosthodontics, München, Germany.

⁵Tenured Associate Professor, Ludwig-Maximilians University Munich, Department of Prosthodontics, München, Germany.

Correspondence to: Dr Peter Gehrke, Bismarckstrasse 27, 67059 Ludwigshafen, Germany. Fax: +49-621-68124468. Email: dr-gehrke@prof-dhom.de

©2015 by Quintessence Publishing Co Inc.

alumina, and zirconia are available for the fabrication of implant abutments.

In the past, two main types of abutments were available for restoring implants: stock abutments, traditionally supplied by dental implant manufacturers to match their respective implant systems, and custom cast abutments. Recently, novel computer-aided design/computer-assisted manufacture (CAD/CAM) abutments were introduced. CAD/CAM abutments can be custom designed to recreate the desired emergence profile and supporting crown orientation, facilitating the formation of anatomical mucosal topography and coronal contours for prosthetic replacement.¹¹ Specific computer software and milling machines utilize scan data from the patient's dental casts to fabricate a computer-generated abutment, milled from a block of titanium or zirconia, without the inaccuracies inherent in the lost-wax method. In general, all metal abutments have been reported to cause a greyish discoloration of the surrounding soft tissues, compromising the esthetic outcome in the anterior arches.^{11,12} This discoloration is most apparent in patients with a thin gingival biotype that is incapable of blocking reflective light from the metallic abutment surface.¹³ Thus, owing to their toothlike color and possible biologic advantages, ceramic abutments have been promoted to achieve better mucogingival esthetics.^{11,14–18} Although a minimal strength value for ceramic abutments has not been defined, clinical studies have demonstrated sufficient fracture resistance of zirconia abutments in the oral cavity for single-tooth replacement in the anterior and premolar regions.^{19,20} Today, zirconia abutments with various implant-abutment connection geometries exist for different implant types. In addition to prefabricated zirconia stock abutments (SZ), one-piece (OP) and two-piece (TP) CAD/CAM zirconia abutments are available. OP abutments, including the implant-abutment connection, are manufactured entirely in a central production process by CAD/CAM technology. TP abutments consist of a prefabricated insert base of titanium to which a customized CAD/CAM zirconia coping is cemented in the laboratory (hybrid abutments). Recent *in vitro* studies have demonstrated that the geometry of the implant-abutment connection has a critical influence on the technical outcome of zirconia abutments.^{21–24} Significantly higher bending moments were achieved for CAD/CAM zirconia abutments with internal connections via a secondary titanium insert (TP) than for abutments with external connections. Therefore, the use of a secondary titanium insert may be beneficial for the stability of zirconia abutments.

Limited data are available for the *in vivo* and *in vitro* performance of implant-supported restorations on TP CAD/CAM zirconia implant abutments. Therefore, the



Fig 1 Control and test abutments with 15 degrees of angulation. *Left to right*: control group (SZ, unprepared stock zirconia abutment, Xive CERCON); test group 1 (OP CAD/CAM zirconia abutment, Compartis); test group 2 (TP CAD/CAM zirconia abutment, Compartis).

current study was performed to investigate the fatigue and fracture resistance of TP CAD/CAM zirconia abutments and to compare these results to those for OP CAD/CAM and commercially available SZ abutments. The working hypothesis of the study was that the fracture resistance of TP CAD/CAM zirconia implant abutments is higher than the fracture load of OP CAD/CAM zirconia and SZ abutments.

MATERIALS AND METHODS

Power Analysis

To determine the required sample size, a post hoc power analysis was performed according to Fan et al²⁵ (BiAS 10.0, Windows, Microsoft). The power calculation revealed that seven abutments in each group (21 total) were necessary to reach a statistical power of 80% with a .05 level of significance.

Specimen Fabrication

Twenty-one abutment-crown specimens were prepared for three test groups of seven specimens each representing implant-supported anterior single restorations. Control group 1 (SZ) consisted of specimens with identical, unprepared SZ abutments (CERCON Dentsply Implants, 3.8 mm diameter, 15-degree angle, Dentsply Implants), test group 2 (OP) had specimens with identical OP CAD/CAM zirconia abutments (Compartis DeguDent, 3.8 mm diameter, 15-degree angle, DeguDent), and test group 3 (TP) had specimens with identical TP CAD/CAM zirconia abutments (XIVE Ti-Base, 3.8 mm diameter, Dentsply Implants; and zirconia coping, 15-degree angle; Compartis DeguDent, DeguDent) (Fig 1).



Fig 2 Simplified zirconia CAD/CAM crowns (CERCON) with 30-degree occlusal plane and occlusal screw access adhesively bonded to test abutments (left to right: SZ, OP, TP).

A clinical case in which the maxillary right central incisor had been replaced with a XiVE S implant (Dentsply Implants) was selected to digitally design a master abutment with 15 degrees angulation using special abutment design software (CERCON Art, DeguDent). The peri-implant mucosa for this particular patient had been conditioned with an implant-supported provisional restoration, resulting in a scalloped soft tissue margin.

Prior to designing the CAD abutment, a scan abutment was mounted on the implant replica of the master cast and scanned (CERCON Art, DeguDent). All CAD/CAM abutments (OP, TP) were designed so that the prospective crown margin would follow the mucosa scallop with a slightly submucosal shoulder. For the TP group, the bonding surfaces of the titanium inserts and zirconia ceramic copings were airborne particle-abraded with 50- μ m aluminum oxide particles at a pressure of 2.0 bar (0.25 MPa) for 20 seconds at a distance of 10 mm (P-G 400, Harnisch & Rieth) and then cleaned in 96% isopropyl alcohol for 3 minutes.

Then, the pretreated surfaces of the titanium inserts and the inner part of the zirconia copings received a single-component primer to promote adhesion between the luting areas (Monobond Plus, Ivoclar Vivadent). The bonding agent was applied with a microbrush and allowed to react for 60 seconds before being dispersed by a stream of air. All specimens were bonded with a resin-based luting agent (Multilink Implant, Ivoclar Vivadent) by the same operator according to the manufacturer's instructions. The copings were seated with a device that allowed a defined load of 5 kg to be applied along the longitudinal axis of the abutment for a 10-minute period. Excess resin was removed from the bonding margins before it set completely and the assembly was then light-cured for 60 seconds (Heliomat, Ivoclar Vivadent) according to the manufacturer's recommendations. The SZ abutments



Fig 3 Twenty-one geometrically identical, simplified zirconia crowns (CERCON) for the allocated control and test abutments (XiVE S, 3.8 mm in diameter).

were left unprepared to minimize variability in abutment size and thickness and to eliminate the weakening effect of grinding the abutments.

Twenty-one geometrically identical, simplified CAD/CAM crowns with occlusal screw access and an occlusal plane of 30 degrees were milled from zirconia (CERCON Brain Smart Ceramics, DeguDent) for the allocated control and test abutments. After milling, all crowns were adhesively cemented to the abutments with a self-curing resin composite cement (Panavia F, Kuraray Europe) according to the manufacturer's instructions (Figs 2 and 3).

After specimen fabrication, 21 implants of commercially pure grade 4 titanium with a diameter of 3.8 mm and length of 13 mm (XiVE S, Dentsply Implants) were embedded perpendicularly in a block of self-curing resin (DPC-Resin LT 2, Duroplat-Chemie Vertriebs). The implant shoulder extended the level of the surrounding material by 2 mm, simulating crestal bone resorption. After the implants were embedded, the abutment-crown combinations were joined to the implants with a new titanium abutment screw and torqued to 20 Ncm, as recommended by the manufacturer. A calibrated electronic implant torque controller (Intrasurg, Kavvo) was used to ensure proper seating torque for all abutments.

Dynamic Loading

All 21 specimens were thermocycled and loaded simultaneously in a dual-axis chewing simulator that combined thermocycling and fatigue testing (CS-4, SD). The specimens were fixed on a loading platform at 30 degrees off-axis, and cyclic fatigue loading was applied to the tapered occlusal area of each simplified crown with a round stainless steel stylus with a diameter of 3.5 mm (Fig 4). The dynamic loading included an additional horizontal sliding motion of 2 mm, perpendicular to the implant axis to induce bending moments at

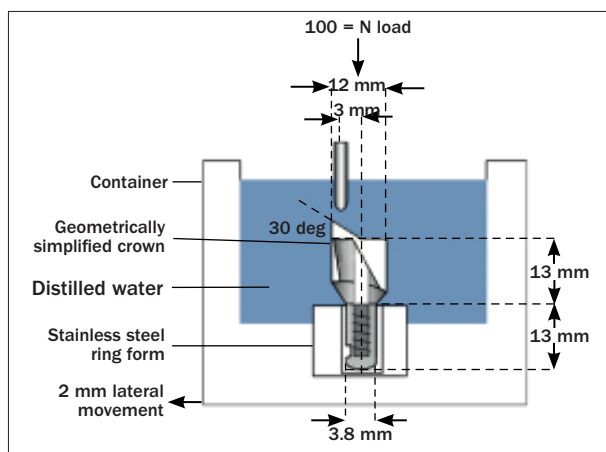


Fig 4 Schematic of dynamic loading test setup in a single chewing chamber.

the implant-abutment interface. A force of 100 N was applied for 120,000 cycles at a frequency of 1.2 Hz. The loading speed was 10 mm/s, and the lifting speed was 60 mm/s. Simultaneously, 1,000 thermal cycles from 5°C to 55°C for 30 seconds each were performed.

Fracture Resistance Testing

Finally, all of the specimens were tested for fracture resistance using a universal testing machine (Zwick Roell 1445, Zwick). The maximum load was applied to the tapered occlusal area for each crown at an angle of 30 degrees relative to the implant axis with a crosshead speed of 0.5 mm/min until the implant-abutment connection failed. Tin foil, 0.5 mm thick, was placed between the stylus and crown to ensure an even distribution of forces across the specimens (DENTAURUM). The software associated with the universal testing machine (TestXpert 3.2, Zwick) recorded the applied force in relation to the deformation of the abutment screw or fracture of the abutment. The type of failure mode and load required until failure were recorded.

The key outcome parameter for the stress experiments was the fracture load. For the SZ and OP groups, the load-displacement diagram indicated a fracture with a sharp drop (black line in Fig 5); therefore, the fracture load could be determined in a straightforward manner as the highest force measured during the cycle. In contrast, no externally visible destruction of the abutments occurred in the stress experiments with the TP group. However, there was a clearly visible transition from a quasilinear to a flattened, more irregular curve, indicating irreversible deformation of parts of the abutment (green line in Fig 5), and the force applied at the transition point was recorded as the fracture strength in this group.

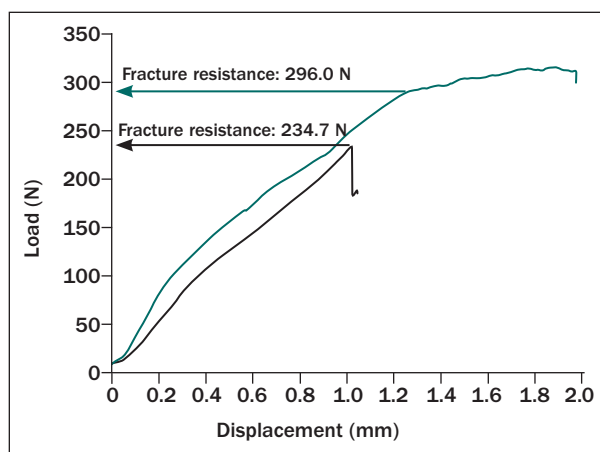


Fig 5 Examples of load-displacement diagrams of SZ (#7) and TP (#4) abutments. In the SZ (one-piece) abutment, the maximum recorded force equals the fracture resistance (here, 234.7 N), whereas in the TP abutment, the fracture resistance reading can be taken at the transition from the quasilinear to the flattened, more irregular curve.

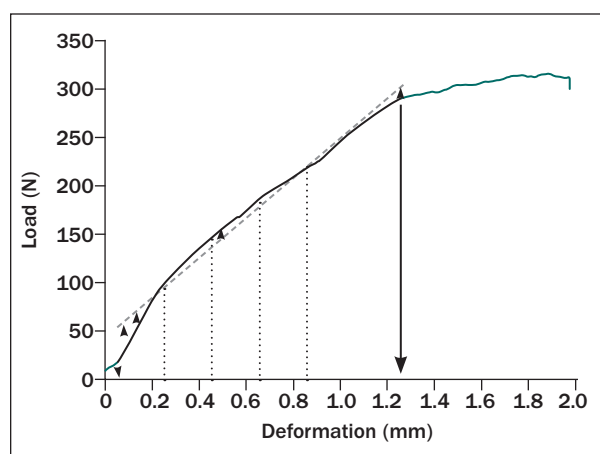


Fig 6 Schematic stress-strain diagram (TP #3). Black field = reversible elastic deformation; green field = irreversible plastic deformation. The black arrow at right indicates the transition from elastic to plastic deformation.

In addition to the fracture resistance, the following three additional parameters characterizing the dynamic deformation of the abutments were determined from load-displacement diagrams (Fig 6):

1. Maximum deformation: the amount of displacement at the breaking point (solid black arrows in Fig 6)
2. Stiffness: the gradient of the linear slope calculated for individual load-displacement diagrams (dashed line in Fig 6)
3. Mean deviation of the actual load-displacement diagram from the calculated linear slope (arithmetic mean of the distance at all recorded points and at predefined intervals of 0.2, 0.4, 0.6, and 0.8 mm, denoted by the dotted lines in Fig 6)



Figs 7a to 7c Types of failure of the abutments. (a) Prefabricated (SZ #4), (b) OP CAD/CAM (#3), (c) TP CAD/CAM (#3). Note the bent screw at the TP abutment.

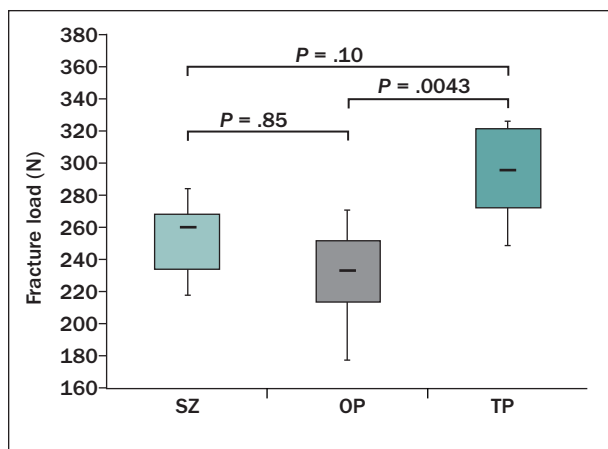


Fig 8 Fracture loads of abutments in the three groups. Shown are 10th percentile (lower whisker), 25th percentile (lower box margin), median (center line), 75th percentile (upper box margin), and 90th percentile (upper whisker).

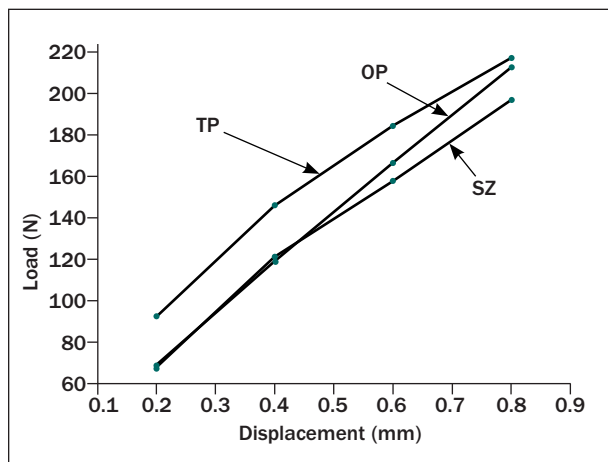


Fig 9 Applied load at predefined points of displacement in the three test groups (mean values).

Statistical Analysis

The results were analyzed using the Statistical Package for the Social Sciences Version 20 (SPSS Inc). The level of significance was set at 5% ($P < .05$) for all applied statistical tests. Kolmogorov-Smirnov and Shapiro-Wilk

tests were used to test the normality of data distribution. All groups were normally distributed. Therefore, parametric descriptive statistics were computed. One-way analysis of variance followed by Scheffé post hoc test was used to determine the significance of differences between the tested groups.

RESULTS

Types of Abutment Failure

In the SZ and OP groups, all of the abutments failed and fractured into two or more fragments after testing of the load-bearing capacity. All fractures occurred below the implant shoulder. None of the abutments in the TP group displayed apparent disintegration, but the failure was evident by bending of the retaining screw, which corresponded with the flattening of the load-displacement curves (Fig 5). Figure 7 shows examples of fractured abutments.

Comparison of Fracture Resistance

OP CAD/CAM abutments (232.1 ± 29.8 N) and SZ abutments (251.8 ± 23.2 N) showed appreciably lower fracture loads than the TP CAD/CAM abutments (291.4 ± 27.8 N). While analysis of variance demonstrated a significant influence of abutment construction on fracture resistance ($P = .0052$), the paired post hoc comparisons of SZ vs OP and SZ vs TP yielded no significance (Scheffé test, $P = .85$ and $P = .10$, respectively). The difference between TP and OP remained statistically significant ($P = .0043$) (Fig 8).

The Relationship Between Load and Displacement

At predefined points of displacement, the abutments in the TP group displayed a fairly consistent difference of approximately 20 to 30 N compared to the SZ group; in contrast, the OP group roughly connected the starting point of the SZ and the finishing point of the OP group (ie, it exhibited a noticeably steeper incline in the load-displacement diagram) (Fig 9).

Table 1 Load-Displacement Calculations (Means \pm Standard Deviations)

Parameter	Group SZ	Group OP	Group TP	Significance
Maximum deformation (mm)	1.11 \pm 0.16	0.91 \pm 0.16	1.32 \pm 0.24	SZ vs OP, ns SZ vs TP, ns OP vs TP, $P < .01$
Deformation at different points (N)				
At 0.2 mm	67.7 \pm 16.4	68.7 \pm 20.9	92.7 \pm 12.6	SZ vs OP, ns SZ vs TP, $P < .05$ OP vs TP, ns
At 0.4 mm	121.3 \pm 19.8	119.0 \pm 21.8	146.2 \pm 9.8	SZ vs OP, ns SZ vs TP, $P < .05$ OP vs TP, $P < .05$
At 0.6 mm	158.2 \pm 22.2	166.7 \pm 16.8	184.9 \pm 10.4	SZ vs OP, ns SZ vs TP, $P < .05$ OP vs TP, ns
At 0.8 mm	197.6 \pm 32.6	213.1 \pm 21.3	217.7 \pm 9.0	SZ vs OP ns SZ vs TP, ns OP vs TP, ns
Incline of linear slope (N/mm)	214.5 \pm 46.9	237.1 \pm 28.2	196.8 \pm 28.4	SZ vs OP, ns SZ vs TP, ns OP vs TP, $P = .084$
Mean deviation of actual values from the linear slope (N)	6.53 \pm 2.09	6.00 \pm 3.62	9.94 \pm 2.58	SZ vs OP, ns SZ vs TP, ns OP vs TP, $P < .05$

The results of the load-displacement calculations are shown in Table 1. The maximum deformation before fracture was highest in the TP group (1.32 \pm 0.24 mm; range, 1.11 to 1.73 mm), followed by the SZ group (1.11 \pm 0.16 mm; range, 0.90 to 1.34 mm) and the OP abutments (0.91 \pm 0.16 mm; range, 0.73 to 1.19 mm). Therefore, the highest deformation before fracture in the OP group was a mere 0.08 mm larger than the lowest deformation in the TP group (ie, the ranges were almost mutually exclusive). Nevertheless, the difference between the two groups was statistically significant.

Accordingly, the force required to deform the TP abutments by a prespecified margin was consistently higher than that for the SZ and OP groups (compare Fig 9). Because of the aforementioned approximation of the OP and TP slopes at higher displacements, the incline of the linear slope was highest in the OP group, and a statistically significant difference was seen mainly between SZ and TP with respect to the force required to deform the TP abutments by a prespecified margin.

The deviation of the actual values from the calculated linear slope was highest in the TP group (9.94 \pm 2.58 N) and lowest in the OP group (6.00 \pm 3.62 N), with the SZ group falling in between the two experimental groups (6.53 \pm 2.09 N).

In summary, the OP abutments were less resistant to deformation and fracture but more consistent and predictable with respect to their load-displacement behavior than the TP abutments. The OP abutments exhibited lower fracture resistance but better resistance to subfracture deformation compared to the SZ

abutments, whereas the TP abutments demonstrated superior characteristics compared to the SZ abutments in all aspects, with the exception of deformation predictability.

DISCUSSION

Within the limitations of this investigation, the study hypothesis can be confirmed, as the TP abutments exhibited a significantly higher fracture resistance than the OP and SZ abutments. A force-displacement analysis yielded compatible results. The SZ abutments displayed a certain advantage because their failure was more predictable; however, failure occurred under considerably lower displacement forces compared to the TP abutments. Although they were structurally similar, OP and SZ abutments displayed contrasting behavior regarding fracture resistance. Despite the fact that both abutment types—including their implant-abutment connection—were made entirely of zirconia, the OP abutments exhibited lower fracture strength but a higher stability against subfracture compared to the SZ abutments. Possible causes could be related to the precision of the respective fabrication processes and/or the quality of the raw zirconia material being used. Whereas the abutment shoulders of the OP group were individually CAD/CAM designed and manufactured to follow the given peri-implant mucosa scallop, the SZ abutments were left unprepared to eliminate any weakening effect of grinding

after industrial production. Therefore, the shape and dimensions of the abutments in these two test groups (OP, SZ) were not identical, which could have possibly affected their fracture resistance behavior. The higher fracture resistance of the TP abutments compared to the OP and SZ specimens is mechanically explicable, and similar findings have been reported previously.²³ All-ceramic abutments cannot be machined to the same degree of precision as metal abutments. Recent studies have shown that one-piece zirconia abutments have a marginal misfit with implants that might cause screw loosening, micromotion, wear of the implant-abutment interface, and a larger marginal gap subject to bacterial colonization.^{12,19,26}

In relation to the bite forces occurring during occlusal function, the load stability of the abutments under investigation in the present study is favorable. The chewing forces in the axial direction typically do not exceed 220 N²⁷; thus, the tested abutments should withstand functional loading, even in an angled position. However, the fracture load of the OP abutments (with a mean of approximately 230 N) is relatively close to the typical chewing force; moreover, the maximum bite forces during regular occlusal function can reach 150 to 400 N in the anterior and 1,000 N in the posterior area of the jaws.²⁸⁻³³ Therefore, it is recommended that clinicians err on the side of caution and avoid OP all-ceramic abutments in the posterior region.

The limiting factor in the failure of ceramic abutments is not the type of crown fixation or luting gap in TP abutments but the bending of the ceramic structure itself; according to studies by Att et al^{26,34} and Truninger et al,²¹ a failure threshold of approximately 400 N can be assumed. Two different failure patterns were observed in the present *in vitro* investigation. Whereas fractures of all-zirconia abutments (OP, SZ) always began within the ceramic, failures of the TP specimens were always located in the abutment screw, which thus represented the weakest component. However, possible deformation of the implant and/or wear of the implant-abutment interface were not explored in the present investigation.

Abutment fractures are a rare but potentially devastating complication in implant dentistry. It is difficult to determine an incidence because most clinical trials report no abutment fractures at all; however, a cursory search of the literature revealed that abutment fractures do indeed occur sporadically.³⁵⁻³⁷ Therefore, fracture resistance of abutments is clearly an important issue.

A comparison of the results to different studies would be helpful in providing pertinent recommendations for the use of different types of all-ceramic abutments. However, such a comparison is restricted by methodologic differences among trials: whereas

there is ample published evidence, there are many differences in experimental settings (eg, fatigue cycle number and conditions, angulation and method of force application, choice of outcome parameters). Therefore, valid comparisons are mainly restricted to differences between the materials and constructions within a single study. For example, important differences have been shown with respect to abutment material,^{22,24,26,34,38-45} model,⁴⁶⁻⁴⁸ manufacturing technique (CAD/CAM vs prefabricated),⁴⁹ luting and bonding agents,⁵⁰ amount of external axial reduction,⁵¹ and abutment angulation.^{52,53}

In most trials that investigated the fracture load, the reported forces were noticeably higher than in the present study (typically in the range of 400 to 800 N^{21,22,26,34,42,44,46,47,51} or more^{45,48}), but similar⁵⁴ and even lower values^{38,39} have also been reported. Moreover, there are substantial variations between studies, and these variations are likely attributable to differences in methodology rather than the actual fracture load of the abutments.

The very limited possibility of comparing results between studies can be easily illustrated with the fracture loads reported for different abutment materials. Whereas Foong et al³⁸ reported fractures in titanium abutments at a mean load of 270 N and ceramic abutments at 140 N, the fracture loads reported by Att et al^{26,34} for titanium and ceramic abutments exceeded 1,200 and 440 N, respectively.

One of the most important experimental factors is the number of load cycles exerted during fatigue testing. A previous study¹⁶ found that all-ceramic abutments displayed an almost ideal logarithmic relationship between the number of load cycles and fracture resistance, allowing for a fairly accurate prediction of further structural weakening with an increasing number of cycles. Another crucial factor for simple physical bearing on the recorded load is the angle of the tapered part of the experimental setup⁵⁵ (30 degrees in the present study; see Fig 2). For future studies, the conditions for cyclic loading and loading angle should be standardized to obtain information that is comparable across studies. Simulating functional loading of endosseous dental implants and their abutment components under worst-case conditions, the coronal ends of the implants in the current study extended 2 mm above the level of the surrounding material to create a situation of crestal bone resorption.

A further aspect that should be respected is the wear effect. This has been demonstrated at the implant-abutment interface when zirconia and titanium are brought into direct contact.^{56,57}

Despite the impressive success of implant dentistry, there are still issues to be addressed through systematic research, and one of the most notable areas

of demand is the clinical long-term success of zirconia abutments on implants.^{19,56} Although the suitability of zirconia CAD/CAM abutments as such is hardly debatable, the published results of stress testing are extremely variable,⁵⁷ making comparisons difficult. A more comprehensive understanding of the mechanical properties of different systems would be helpful to preemptively secure the long-term success of implant-supported restorations on CAD/CAM all-ceramic abutments. Meanwhile, the esthetic benefit of all-ceramic abutments in posterior areas must be carefully balanced against the reduced fracture resistance compared to titanium abutments.

CONCLUSIONS

- Two-piece abutments with an internal-hex connection demonstrated greater resistance to fracture compared to one-piece and stock zirconia abutments.
- Two-piece abutments might be clinically beneficial in high-load areas, such as premolar and molar single-tooth replacements.

ACKNOWLEDGMENTS

The authors gratefully acknowledge Dr Hartmut Buhck for his contribution to data analysis, Dr Kurt Erdelt and Gerlinde Lange for their technical support, and Mr André Spanel for his assistance during the review process. The authors declare no conflicts of interest. Dentsply Implants and DeguDent generously supported the study with implants and abutments.

REFERENCES

- Esposito M, Maghahre H, Grusovin MG, Ziounas I, Worthington HV. Interventions for replacing missing teeth: Management of soft tissues for dental implants. *Cochrane Database Syst Rev* 2012;2: CD006697.
- Esposito M, Maghahre H, Grusovin MG, Ziounas I, Worthington HV. Soft tissue management for dental implants: What are the most effective techniques? A Cochrane systematic review. *Eur J Oral Implantol* 2012;5:221–238.
- Lang NP, Pun L, Lau KY, Li KY, Wong MC. A systematic review on survival and success rates of implants placed immediately into fresh extraction sockets after at least 1 year. *Clin Oral Implants Res* 2012; 23(suppl 5):39–66.
- Meijer HJ, Stellingsma K, Meijndert L, Raghoobar GM. A new index for rating aesthetics of implant-supported single crowns and adjacent soft tissues—The Implant Crown Aesthetic Index. *Clin Oral Implants Res* 2005;16:645–649.
- Lang NP. A quarter of a century as a trendsetter in implant dentistry. *Clin Oral Implants Res* 2014;25:1–2.
- Shavell HM. The periodontal-restorative interface in fixed prosthodontics: Tooth preparation, provisionalization, and biologic final impressions—Part II. *Pract Periodontics Aesthet Dent* 1994;6:49–60.
- Shavell HM. The periodontal-restorative interface in fixed prosthodontics: Tooth preparation, provisionalization, and biologic final impressions. Part I. *Pract Periodontics Aesthet Dent* 1994;6:33–44.
- Welander M, Abrahamsson I, Berglundh T. The mucosal barrier at implant abutments of different materials. *Clin Oral Implants Res* 2008;19:635–641.
- Brånemark P-I. Introduction to osseointegration. In: Brånemark P-I, Zarb GA, Albrektsson T (eds). *Tissue-Integrated Prosthesis: Osseointegration in Clinical Dentistry*. Chicago: Quintessence, 1985:11–76.
- Abrahamsson I, Berglundh T, Glantz PO, Lindhe J. The mucosal attachment at different abutments. An experimental study in dogs. *J Clin Periodontol* 1998;25:721–727.
- Sailer I, Zembic A, Jung RE, Hämmerle CH, Mattioli A. Single-tooth implant reconstructions: Esthetic factors influencing the decision between titanium and zirconia abutments in anterior regions. *Eur J Esthet Dent* 2007;2:296–310.
- Brodbeck U. The ZiReal Post: A new ceramic implant abutment. *J Esthet Restorative Dent* 2003;15:10–23.
- Park SE, Da Silva JD, Weber HP, Ishikawa-Nagai S. Optical phenomenon of peri-implant soft tissue. Part I. Spectrophotometric assessment of natural tooth gingiva and peri-implant mucosa. *Clin Oral Implants Res* 2007;18:569–574.
- Dede DÖ, Armaganci A, Ceylan G, Cankaya S, Celik E. Influence of abutment material and luting cements color on the final color of all ceramics. *Acta Odontol Scand* 2013;71:1570–1578.
- Degidi M, Artese L, Scarano A, Perrotti V, Gehrke P, Piattelli A. Inflammatory infiltrate, microvessel density, nitric oxide synthase expression, vascular endothelial growth factor expression, and proliferative activity in peri-implant soft tissues around titanium and zirconium oxide healing caps. *J Periodontol* 2006;77:73–80.
- Gehrke P, Dhom G, Brunner J, Wolf D, Degidi M, Piattelli A. Zirconium implant abutments: Fracture strength and influence of cyclic loading on retaining-screw loosening. *Quintessence Int* 2006; 37:19–26.
- Sailer I, Zembic A, Jung RE, Siegenthaler D, Holderegger C, Hämmerle CH. Randomized controlled clinical trial of customized zirconia and titanium implant abutments for canine and posterior single-tooth implant reconstructions: Preliminary results at 1 year of function. *Clin Oral Implants Res* 2009;20:219–225.
- Zembic A, Sailer I, Jung RE, Hämmerle CH. Randomized-controlled clinical trial of customized zirconia and titanium implant abutments for single-tooth implants in canine and posterior regions: 3-year results. *Clin Oral Implants Res* 2009;20:802–808.
- Nakamura K, Kanno T, Milleding P, Ortengren U. Zirconia as a dental implant abutment material: A systematic review. *Int J Prosthodont* 2010;23:299–309.
- Zembic A, Bosch A, Jung RE, Hämmerle CH, Sailer I. Five-year results of a randomized controlled clinical trial comparing zirconia and titanium abutments supporting single-implant crowns in canine and posterior regions. *Clin Oral Implants Res* 2013;24:384–390.
- Truninger TC, Stawarczyk B, Leutert CR, Sailer TR, Hämmerle CH, Sailer I. Bending moments of zirconia and titanium abutments with internal and external implant-abutment connections after aging and chewing simulation. *Clin Oral Implants Res* 2012;23:12–18.
- Kim JS, Raigrodski AJ, Flinn BD, Rubenstein JE, Chung KH, Mancl LA. In vitro assessment of three types of zirconia implant abutments under static load. *J Prosthet Dent* 2013;109:255–263.
- Sailer I, Sailer T, Stawarczyk B, Jung RE, Hämmerle CH. In vitro study of the influence of the type of connection on the fracture load of zirconia abutments with internal and external implant-abutment connections. *Int J Oral Maxillofac Implants* 2009;24:850–858.
- Mühlmann S, Truninger TC, Stawarczyk B, Hämmerle CH, Sailer I. Bending moments of zirconia and titanium implant abutments supporting all-ceramic crowns after aging. *Clin Oral Implants Res* 2014;25:74–81.
- Fan C, Zhang D, Zhang CH. On sample size of the Kruskal-Wallis test with application to a mouse peritoneal cavity study. *Biometrics* 2011;67:213–224.
- Att W, Kurun S, Gerds T, Strub JR. Fracture resistance of single-tooth implant-supported all-ceramic restorations: An in vitro study. *J Prosthet Dent* 2006;95:111–116.
- Proeschel PA, Morneburg T. Task-dependence of activity/bite-force relations and its impact on estimation of chewing force from EMG. *J Dent Res* 2002;84:464–468.

28. Varga S, Spalj S, Lapter Varga M, Anic Milosevic S, Mestrovic S, Slaj M. Maximum voluntary molar bite force in subjects with normal occlusion. *Eur J Orthod* 2011;33:427–433.
29. Kamegai T, Tatsuki T, Nagano H, et al. A determination of bite force in northern Japanese children. *Eur J Orthod* 2005;27:53–57.
30. Fontijn-Tekamp FA, Slagter AP, Van Der Bilt A, et al. Biting and chewing in overdentures, full dentures, and natural dentitions. *J Dent Res* 2000;79:1519–1524.
31. Alkan A, Keskiner I, Arici S, Sato S. The effect of periodontal surgery on bite force, occlusal contact area and bite pressure. *J Am Dent Assoc* 2006;137:978–983.
32. Haraldson T, Carlsson GE, Ingervall B. Functional state, bite force and postural muscle activity in patients with osseointegrated oral implant bridges. *Acta Odontol Scand* 1979;37:195–206.
33. Paphangkorakit J, Osborn JW. The effect of pressure on a maximum incisal bite force in man. *Arch Oral Biol* 1997;42:11–17.
34. Att W, Kurun S, Gerds T, Strub JR. Fracture resistance of single-tooth implant-supported all-ceramic restorations after exposure to the artificial mouth. *J Oral Rehabil* 2006;33:380–386.
35. Andersson B, Taylor A, Lang BR, et al. Alumina ceramic implant abutments used for single-tooth replacement: A prospective 1- to 3-year multicenter study. *Int J Prosthodont* 2001;14:432–438.
36. Davó R, Pons O. Prostheses supported by four immediately loaded zygomatic implants: A 3-year prospective study. *Eur J Oral Implants Res* 2013;6:263–269.
37. Vroom MG, Sipos P, de Lange GL, et al. Effect of surface topography of screw-shaped titanium implants in humans on clinical and radiographic parameters: A 12-year prospective study. *Clin Oral Implants Res* 2009;20:1231–1239.
38. Foong JK, Judge RB, Palamara JE, Swain MV. Fracture resistance of titanium and zirconia abutments: An in vitro study. *J Prosthet Dent* 2013;109:304–312.
39. Kohal RJ, Finke HC, Klaus G. Stability of prototype two-piece zirconia and titanium implants after artificial aging: An in vitro pilot study. *Clin Implant Dent Relat Res* 2009;11:323–329.
40. Leutert CR, Stawarczyk B, Truninger TC, Hämmerle CH, Sailer I. Bending moments and types of failure of zirconia and titanium abutments with internal implant-abutment connections: A laboratory study. *Int J Oral Maxillofac Implants* 2012;27:505–512.
41. Oderich E, Boff LL, Cardoso AC, Magne P. Fatigue resistance and failure mode of adhesively restored custom implant zirconia abutments. *Clin Oral Implants Res* 2012;23:1360–1368.
42. Sghaireen MG. Fracture resistance and mode of failure of ceramic versus titanium implant abutments and single implant-supported restorations. *Clin Implant Dent Relat Res* 2013 Oct 9. [Epub ahead of print]
43. Vigolo P, Fonzi F, Majzoub Z, Cordioli G. An in vitro evaluation of titanium, zirconia, and alumina Procera abutments with hexagonal connection. *Int J Oral Maxillofac Implants* 2006;21:575–580.
44. Wang CF, Huang HL, Lin DJ, Shen YW, Fuh LJ, Hsu JT. Comparisons of maximum deformation and failure forces at the implant-abutment interface of titanium implants between titanium-alloy and zirconia abutments with two levels of marginal bone loss. *Biomed Eng Online* 2013;12:45.
45. Wolf D, Bindl A, Schmidlin PR, Luthy H, Mormann WH. Strength of CAD/CAM-generated esthetic ceramic molar implant crowns. *Int J Oral Maxillofac Implants* 2008;23:609–617.
46. Kerstein RB, Radke J. A comparison of fabrication precision and mechanical reliability of 2 zirconia implant abutments. *Int J Oral Maxillofac Implants* 2008;23:1029–1036.
47. Protopapadaki M, Monaco EA Jr, Kim HI, Davis EL. Comparison of fracture resistance of pressable metal ceramic custom implant abutment with a commercially fabricated CAD/CAM zirconia implant abutment. *J Prosthet Dent* 2013;110:389–396.
48. Steinebrunner L, Wolfart S, Ludwig K, Kern M. Implant-abutment interface design affects fatigue and fracture strength of implants. *Clin Oral Implants Res* 2008;19:1276–1284.
49. Hamilton A, Judge RB, Palamara JE, Evans C. Evaluation of the fit of CAD/CAM abutments. *Int J Prosthodont* 2013;26:370–380.
50. Gehrke P, Alius J, Fischer C, Erdelt KJ, Beuer F. Retentive strength of two-piece CAD/CAM zirconia implant abutments. *Clin Implant Dent Relat Res* 2014;16:920–925.
51. Adatia ND, Bayne SC, Cooper LF, Thompson JY. Fracture resistance of yttria-stabilized zirconia dental implant abutments. *J Prosthodont* 2009;18:17–22.
52. Canullo L, Coelho PG, Bonfante EA. Mechanical testing of thin-walled zirconia abutments. *J Appl Oral Sci* 2013;21:20–24.
53. Ellakwa A, Raj T, Deeb S, Ronaghi G, Martin FE, Klineberg I. Influence of implant abutment angulations on the fracture resistance of overlaying CAM-milled zirconia single crowns. *Aust Dent J* 2011;56:132–140.
54. Nothdurft FP, Doppler KE, Erdelt KJ, Knauber AW, Pospiech PR. Influence of artificial aging on the load-bearing capability of straight or angulated zirconia abutments in implant/tooth-supported fixed partial dentures. *Int J Oral Maxillofac Implants* 2010;25:991–998.
55. Yang J, Wang K, Liu G, Wang D. Fracture resistance of inter-joined zirconia abutment of dental implant system with injection molding technique. *Clin Oral Implants Res* 2013;24:1247–1250.
56. Gomes AL, Montero J. Zirconia implant abutments: A review. *Med Oral Patol Oral Cir Bucal* 2011;16:e50–55.
57. Velázquez-Cayón R, Vaquero-Aguilar C, Torres-Lagares D, Jiménez-Melendo M, Gutiérrez-Pérez JL. Mechanical resistance of zirconium implant abutments: A review of the literature. *Med Oral Patol Oral Cir Bucal* 2012;17:e246–250.